A Novel Microdevice for Rapid Neutrophil Purification and Phenotyping in Type 2 Diabetes Mellitus

Tay, Hui Min; Dalan, Rinkoo; Li, Holden King Ho; Boehm, Bernhard Otto; Hou, Han Wei

2017

Tay, H. M., Dalan, R., Li, H. K. H., Boehm, B. O., & Hou, H. W. (2017). A Novel Microdevice for Rapid Neutrophil Purification and Phenotyping in Type 2 Diabetes Mellitus. Small, 14(6), 1702832-.

https://hdl.handle.net/10356/87040

https://doi.org/10.1002/smll.201702832

Article type: Full Paper

A Novel Microdevice for Rapid Neutrophil Purification and Phenotyping in Type 2 Diabetes Mellitus

Hui Min Tay, Rinkoo Dalan, King Ho Holden Li, Bernhard O. Boehm and Han Wei Hou**

Ms. H.M. Tay, Prof. B.O. Boehm, Dr. H.W. Hou
Lee Kong Chian School of Medicine, Nanyang Technological University
11 Mandalay Road, Clinical Sciences Building Level 11, Singapore 308232, Singapore
Email: hwhou@ntu.edu.sg, Bernhard.boehm@ntu.edu.sg

Dr. R. Dalan, Prof. B.O. Boehm
Endocrine and Diabetes, Tan Tock Seng Hospital,
11 Jalan Tan Tock Seng, Singapore 308433, Singapore

Prof. K.H.H. Li
School of Mechanical and Aerospace Engineering, Nanyang Technological University
50 Nanyang Avenue, Block N3, Singapore 639798, Singapore

Keywords: diabetes, neutrophils, blood separation, microfluidics, inflammation

Abstract

Neutrophil dysfunction is strongly linked to type 2 diabetes mellitus (T2DM) pathophysiology, but the prognostic potential of neutrophil biomarkers remains largely unexplored due to arduous leukocyte isolation methods. Herein, we report a novel integrated microdevice for single-step neutrophil sorting and phenotyping (chemotaxis and formation of neutrophil extracellular traps (NETosis)) using small blood volumes (fingerprick). Untouched neutrophils are purified on-chip from whole blood directly using biomimetic cell margination and affinity-based capture, and are exposed to pre-loaded chemoattractant or NETosis stimulant to initiate chemotaxis or NETosis, respectively. Device performance was first characterized using healthy and *in vitro* inflamed blood samples (TNF-α, high glucose), followed by clinical risk stratification in a cohort of subjects with T2DM. Interestingly, "high-risk" T2DM patients characterized by severe chemotaxis impairment revealed significantly higher C-reactive protein (CRP) levels and poor lipid metabolism characteristics as compared to "low-risk" subjects, and their neutrophil chemotaxis responses could be mitigated after *in vitro* metformin treatment. Overall, this unique and user-friendly microfluidics immune health profiling strategy can significantly aid the quantification of chemotaxis and NETosis in clinical settings, and be further translated into a tool for risk stratification and precision medicine methods in subjects with metabolic diseases such as T2DM.

Word count: 196

1. Introduction

Diabetes mellitus (DM), a metabolic disorder characterized by chronic hyperglycemia, is a major health burden worldwide with a predicted rise to 360 million by 2030.[1] In subjects with type 2 diabetes mellitus (T2DM), chronic activation of inflammatory pathways has been reported as a result of the energy imbalance, resulting in increased risks of cardiovascular complications.[2,3,4,5] Neutrophils are the most abundant leukocytes in human blood, and are known to play a pivotal role in T2DM pathogenesis as well as its associated vascular complications.[6] Besides increased leukocyte counts[7] and cell morphological changes[8,9] in T2DM patients, clinical studies have reported defective neutrophil functions[10] and phagocytic activities[11] linked with increased susceptibility to bacterial infections.[12] Development of a comprehensive and robust neutrophil phenotyping strategy is therefore essential in the understanding of the pathobiology in diabetes and associated metabolic diseases, and for point-of-care (POC) risk stratification in T2DM patients in addition to well established cardiovascular risk factor HbA1c (glycemic control), blood pressure and lipids evaluation.

Two innate immune system defense mechanisms related to diabetes pathophysiology are neutrophil chemotaxis and formation of neutrophil extracellular traps (NETs). Chemotaxis, the cell's ability to sense and move in response to chemical gradients, has been shown to be highly suppressed in T2DM patients.[13,14] Upon activation or exposure to bacteria, neutrophils secrete NETs (a process known as NETosis) which form a sticky scaffold consisting mainly of decondensed chromatin fibers, granule-derived microbicidal proteases/elastase and cytotoxic molecules (histones).[15] Increased NETosis has recently been reported in T2DM[16] to be associated with tissue damage and delayed wound healing.[17,18] Despite the strong evidences

suggesting a link between neutrophil dysfunction and states of dysmetabolism including T2DM, existing immunoassays are difficult to implement in clinical settings, and the prognostic potential of neutrophil functional biomarkers remains largely unexplored. In addition, neutrophil studies using genomics and proteomic approaches are limited by laborious isolation processes and the need for milliliter volumes of blood (~4 – 8 mL) to purify sufficient protein and nuclei acid content. While these processes have been successfully miniaturized using microfluidics technologies for sample preparation[19] and high-throughput "-omics" analyses,[20] they are still labour intensive and require technical expertise, and thus do not translate easily for bedside testing.

Conventional cell-based chemotaxis assays including Boyden chamber (transwell), Dunn chamber and micropipette assay suffer from poor reproducibility and ill-defined chemical gradients. [21] Due to the unique microscale flow phenomenon, microfluidics chemotaxis devices based on gradient generator, [22] and enclosed chemotactic reservoirs[23,24] have been developed to generate stable chemoattractant gradient, but they require additional neutrophils purification steps (centrifugation, magnetic affinity binding) which can lead to non-specific cell activation.[25] Integrating on-chip neutrophil isolation capabilities from whole blood using mechanical filters[26] and affinity binding[27,28] help preserve neutrophil native conditions, and have been used to study inflammatory responses in patients with burn injury[29] and asthma.[30] Efficient washing is critical in affinity-based devices, and multiple washing steps (highly dependent on user operation) are typically required to remove the large red blood cells (RBCs) background prior chemotaxis assay. [28,30] NETs are quantified based on immunofluorescence, protein and enzymatic assays, and soluble NETosis-associated proteins.[31] A microfluidics NETosis assay is recently

reported,[32] but users have to perform multiple manual washing steps to remove the RBCs, which can interfere with fluorescence-based assay readout.

To overcome aforementioned technical challenges, we herein report a novel microdevice for integrated neutrophil sorting and functional phenotyping from small blood volumes (fingerprick) in a single step. Neutrophils are enriched from whole blood directly based on biomimetic cell margination[33] and affinity-based cell binding.[19] Captured neutrophils are subsequently exposed to pre-loaded chemoattractant or NETosis stimulus for chemotaxis and NETosis quantification, respectively. In our *in vitro* studies, distinct neutrophil chemotaxis suppression and NETosis upregulation were observed in *in vitro* inflamed blood samples (tumor necrosis factor alpha (TNF-α), high glucose), indicating the efficacy of our developed technology for rapid assessment of neutrophil functions. Finally, the translational potential of the developed device was validated in a pilot study of T2DM patients (n=12) where we observed significant impairment of neutrophil chemotaxis. Intriguingly, when the patients were stratified based on chemotactic phenotypes, "high-risk" patients characterized by severe chemotaxis suppression revealed higher C-reactive protein (CRP) levels ($P < 0.05$) and poor lipid metabolic profiles. *In vitro* metformin treatment of T2DM blood samples also led to overall improvement in neutrophil chemotaxis behavior. Taken together, these results suggest chemotaxis and NETosis as novel functional biomarkers for rapid immune health profiling, and the microfluidics technology can be further developed for real-time risk stratification, and timely monitoring of risk-modifying therapeutics in T2DM patients.

2. Results

2.1 Integrated neutrophil sorting and phenotyping biochip

The microdevice is fabricated in polydimethylsiloxane (PDMS) using standard microfabrication and soft lithography. The device consists of a 1 cm long margination channel (20 × 20 μm (w × h)) with 2 side chambers (0.5 cm × 400 μm × 20 μm (l × w × h)) **(Figure. 1A)**. Each side chamber is connected to a larger reservoir (2 mm × 2 mm, highlighted green boxes in Figure. 1A) proximal to the side channel for loading of chemical stimulus for neutrophil assays. Prior experiments, chemoattractant or NETosis stimulus are introduced into the reservoirs by negative pressure, followed by anti-CD66b antibodies surface functionalization. Briefly, the antibodies are loaded into the side outlets of the device, which will flow towards the centre outlet by manually generating a negative pressure. Hence, the connecting side channels and side chambers are functionalized with anti-CD66b antibodies, and there is minimal coating near the chemoattractant reservoir (enclosed space) as confirmed by fluorescence imaging **(Supplementary Figure S1)**. (*see Supplementary information for more details on device fabrication and preparation*). While CD66b is a surface marker for neutrophils and eosinophils, neutrophils are significantly more abundant (~30-fold higher), and potential eosinophil contamination of ~3% is considered negligible in our study. To initiate the assay, human blood sample (~10 – 20 μL) is introduced directly into the device inlet using a syringe pump at 2 μL min^{-1}. As whole blood transverses through the margination channel, deformable RBCs migrate laterally towards the axial centre (Fahraeus effect), resulting in margination of other cell types (platelets and leukocytes) into the smaller side channels (stage 1).[34] Neutrophils sorted into the side chambers are selectively captured on anti-CD66b functionalized surfaces (stage 2), while RBCs and other immune cell types are washed away **(Figure. 1B)**. This results in efficient

neutrophil capture at the entrance of the side chambers due to the sudden decrease in flow speed as the side channel expands into the larger chamber. The highly-enriched neutrophils are then exposed to the preloaded chemoattractant N-Formylmethionyl-leucyl-phenylalanine (fMLP, 200 nM), or calcium ionophore (20 μM) for chemotaxis and NETosis assay, respectively (stage 3) **(Figure. 1C)**.

2.2 Neutrophil sorting using biomimetic cell margination

Cell margination is an *in vivo* microcirculatory phenomenon whereby leukocytes and platelets are pushed laterally towards the vessel periphery due to axial migration of deformable RBCs during flow.[35] Our group has previously applied the margination principle in microfluidics for direct whole blood processing for efficient separation of malaria-infected RBCs,[33] microbes,[34] as well as extracorporeal blood purification.[36,37] As shown in **Figure 2A** and **Supplementary Figure S2**, hemodynamics effects including plasma skimming (separation of cell-free plasma layer) and leukocyte margination were observed in the channel expansion after the margination channel. By varying channel resistance at the outlet bifurcation, each side channel was designed to collect 5% of the volume eluent (consisting mainly of plasma and marginated leukocytes), and majority of the RBCs was collected in the central outlet as waste. Flow cytometry analysis indicated >80% leukocyte (CD45+) separation efficiency for all flow rates tested (~0.5 – 5 μL min^{-1}) **(Figure. 2B)**. With efficient leukocyte collection and RBCs removal, this translated to ~12-fold leukocyte enrichment at the side outlets at 2 μL min^{-1} **(Figure. 2C)**.

2.3 Neutrophil affinity-based capture and enrichment

After removal of bulk RBCs (stage 1), marginated leukocytes and residual RBCs sorted into the smaller side channel would enter the larger chamber, and neutrophils were immediately captured at the anti CD66b-coated surfaces as RBCs and other blood components were continuously washed away (stage 2). As the sample was perfused using a syringe loaded with saline buffer (1x PBS), the saline buffer would continuously flow into the device after all the blood volume had been processed to remove non-specific cell binding at the side chambers **(Figure. S2)**. Fluid flow simulation was in good agreement with the experimental flow profile and neutrophil adhesion pattern at the entrance of the side chamber **(Figure. S3)**. High speed imaging also indicated ~20 fold decrease in channel flow velocity (~451.2 $\mu m\ s^{-1}$) at the entrance of the side chamber, which was important for efficient neutrophil capture at low shear stress conditions (~0.6 $dynecm^{-2}$).[19] Nucleus staining (Hoechst) further confirmed the presence of highly-purified neutrophils in the device based on distinct multi-lobed nucleus **(Figure. 2D, Supplementary Figure. S4)**. For leukocyte differential analysis using flow cytometry, leukocytes were gated based on forward and side scatter signals, and stained for CD66b, CD14 and CD3/19 antibodies to identify neutrophils, monocytes and lymphocytes, respectively. As expected, a significant decrease (~21.8 ± 4.3%, $P < 0.05$) in neutrophil population was observed in the eluent of the side outlets of anti-CD66b-coated devices as compared to inlet sample and uncoated devices, clearly indicating efficient neutrophil affinity-based capture at the side chambers for downstream functional assays **(Figure. 2E)**.

2.4 On-chip neutrophil chemotaxis assay

A key advantage of the developed chemotaxis assay is the highly localized area of captured neutrophils (~200 – 500 cells) near the chemoattractant reservoir at the side chamber **(Figure. 3A)**. This greatly facilitates real-time characterization of chemotaxis phenotype by time-lapse microscopy imaging at a single region of the device. To characterize the formation of diffusion-based chemotactic gradient, we used fluorescein sodium salt (FITC) dye (Mr ~390 Da) which is similar in molecular size as fMLP (Mr ~428 Da), a potent chemotactic peptide derived from bacteria. The fMLP concentration used was 200 nM and was within the working range previously reported to induce strong chemotaxis responses in microfluidics devices.[24,30] After loading FITC into the reservoir, intensity linescans along the side chamber at different timepoints indicated linear and stable diffusion gradient (~7.8% difference between 60 min and 120 min timepoint) for 2 h **(Figure. 3B)**. To initiate cell migration, the biochip containing purified neutrophils from human whole blood was then placed on a microscope equipped with a live cell incubator (maintained at 5% CO_2 and 37°C). Persistent cell migration towards fMLP was observed for healthy neutrophils, and most of the cells were located near to the edge of the fMLP reservoir after 2 h. The chemotaxis zone was ~1000 μm in length, beginning from the connecting side channel (origin) to the edge of the fMLP reservoir (dotted red line). Using cell tracking analysis (ImageJ), we characterized the frequency distribution of the neutrophils along the direction of the chemoattractant (x-axis) at the start (time 0 min) and end (time 120 min) of the chemotaxis assay **(Figure. 3C)**. To evaluate chemotaxis phenotype, 2 cellular functional properties, namely the percentage of migrating cells and the chemotaxis velocity, were measured **(Figure. S5)**. Neutrophil migration described the fraction of cell moving towards the chemoattractant, and was determined based on the number of cells located beyond 500 μm (50%

of the chemotaxis zone) towards the fMLP chamber after 2 h. Cellular motility was quantified by directional chemotaxis velocity calculated based on average displacement between the migrating neutrophil population (black) and initial cell position (grey).

We next tested our device efficacy using healthy (normoglycemia) blood, and blood samples treated with different inflammatory stimulus (TNF-α (10 ng mL^{-1}), glucose (30 mM) and Protein Kinase C (PKC) activator phorbol myristate acetate (PMA 2 nM)) *in vitro*. Efficient neutrophil sorting and capture were achieved for all treated conditions, indicating the potential of the margination device to process blood samples containing native or activated neutrophils. Interestingly, we observed differential attenuation of chemotaxis responses in inflamed neutrophils, with complete inhibition of cell migration in PMA-treated neutrophils **(Supplementary Figure. S6)**. As shown in **Figure. 3D**, majority of the healthy neutrophils (~66.2 ± 12.6%) migrated towards fMLP, while TNF-α and glucose-treated neutrophils exhibited a significant decrease in cell migration (~45%, $P < 0.05$). A decrease in chemotaxis velocity was also observed in TNF-α treated neutrophils (~5.22 ± 0.37 μm min^{-1}, $P < 0.01$) but not glucose treatment (~6.24± 0.49 μm min^{-1}) when compared to healthy neutrophils (~6.27± 0.59 μm min^{-1}) **(Figure. 3E)**. These results were consistent with previous observations reporting suppression of neutrophil chemotaxis during inflammation.[38,39] When we plotted these functional parameters in a 2D scatter plot, distinct chemotaxis phenotypes were observed in healthy, TNF-α, and glucose-treated neutrophils, clearly highlighting the potential of our developed microfluidic device to purify neutrophils from whole blood and quantitatively assess neutrophil dysfunction **(Figure. 3F)**.

2.5 Clinical applications of developed chemotaxis assay

After characterizing the device sorting and chemotaxis assay, we applied the integrated biochip for various clinical applications including 1) assessment of modulatory effects of anti-diabetic (metformin) and lipid-lowering (pravastatin) drugs in chemotaxis, and 2) immune health profiling in T2DM patients. Both drugs have been shown in large clinical trials to exert positive metabolic and vascular effects[40] and we, along with others, have also shown that these drugs can affect neutrophil rolling,[10] chemotaxis and phagocytosis.[41,42] To avoid prior exposure to these medications, we performed our studies by a short-term exposure of blood samples from normoglycemic healthy subjects with metformin (1 mM) or pravastatin (20 μM) for 1 h before use. Cell migration decreased for both drug treatments ($P < 0.05$), while chemotactic velocity was significantly lower ($P < 0.05$) for pravastatin but not metformin **(Figure. 4A, B)**. These observations were similar with previous *in vitro* studies reporting enhanced neutrophil chemotaxis speed with metformin,[41] and suppressed chemotaxis behavior with pravastatin[42], further highlighting the feasibility and importance of probing neutrophil immune functions in POC testing.

In T2DM, patients suffer from chronic hyperglycemia, which results in low-grade inflammation and increased risks of cardiovascular complications.[2,3,4,5] Neutrophil dysfunctions have been previously reported in T2DM patients,[11,14,43] and we sought to characterize chemotaxis phenotype of T2DM patients (n=12, Table S1) using our developed biochip. As shown in **Figure. 4C**, T2DM chemotaxis phenotype were highly heterogeneous and exhibited reduced cell migration and chemotaxis velocity as compared to healthy neutrophils (dotted green box in Figure. 4C). This healthy region was determined based on three standard deviations (SD) from

the geometrical average values obtained from 5 healthy individuals in our study (cell migration: 43.3 to 98.2%, 99% CI; chemotaxis velocity: 5.162 to 7.566 μm min^{-1}, 99% CI), and these ranges were also in accordance with reported fMLP-induced neutrophil migration (~50-70%),[24,28] and chemotactic velocities (~6 – 14 μm min^{-1})[24,28,30] using other microfluidics platforms. Based on their chemotactic phenotype, we further stratified T2DM patients into "high-risk" and "low-risk" groups. High-risk subjects (n=7) had lower neutrophil migration (<20%) and chemotaxis velocity (~3.72 ± 1.78 μm min^{-1}) as compared to low-risk subjects (n=5, ~40-60% migration and chemotaxis velocity of ~5.44 ± 1.53 μm min^{-1}). Interestingly, when we compared established cardiovascular risk factors between both groups, we found that high-risk T2DM subjects had significantly higher C-reactive protein levels (hsCRP), a key marker for low-grade inflammatory state and cardiovascular risk,[44] than low-risk subjects ($P < 0.05$) **(Figure. 4D)**. Other risk factors including fasting glucose, total cholesterol and low-density lipoprotein (LDL) cholesterol levels were also elevated in the high-risk T2DM patients, and high-density lipoprotein (HDL) cholesterol was lower in the same group **(Supplementary Figure. S7)**. Although the differences between both groups were not statistically significant ($P>0.05$) possibly due to the small sample size, the trends were consistent among different risk factors which suggest possible associations among inflammation, metabolic state and neutrophil functions in T2DM patients. Finally, we characterized the effects of *in vitro* metformin treatment on blood samples obtained from 3 T2DM patients (Patient 1-3 are indicated on Figure. 4C), and observed significant upregulation of neutrophil chemotaxis **(Figure. 4E)**. While patient 1 exhibited negligible changes in cell migration and chemotaxis velocity (and remained in the low-risk region), patient 2 and 3 (in the high-risk group) had significant improvement in chemotaxis phenotype with higher neutrophil migration (for patient 2 and 3) and chemotaxis velocity (for

patient 2). Taken together, these results clearly illustrated the clinical impact of the developed biochip for rapid neutrophil chemotaxis phenotyping for inflammatory risk stratification and precision medicine approaches.

2.6 On-chip NETosis assay

Increased NETosis has been recently reported in T2DM,[16,18] which causes tissue damage and delayed wound healing.[17] Herein, we applied the developed microdevice for rapid NETosis assay by loading a NETosis stimulus (calcium ionophore) into the reservoir instead of fMLP. Whole blood samples were stained with a nuclear dye (Hoechst) before injecting into the biochip for neutrophil capture. NETosis is a complex process which involves chromatin decondensation (loss of lobulated nucleus), nuclear degradation (mixing of chromatin and cytoplasmic granular proteins), and finally extracellular DNA release. To quantify the NETosis behavior, live cell fluorescence timelapse imaging was used to monitor nucleus degradation of the purified neutrophils at the side chambers. Upon exposure to the stimulus, neutrophils undergo gradual nucleus degradation (first steps in NETosis), which resulted in DNA leakage into the cytoplasm and the whole cell becoming fluorescent **(Figure. 5A)**. These distinct morphological changes in fluorescence enabled us to easily distinguish and enumerate neutrophils undergoing NETosis **(Figure. 5B)**.[45] As proof-of-concept for diabetes testing, we characterized the NETosis phenotype in healthy and glucose-treated blood, and observed a general increase in NETosis in glucose-treated neutrophils over time ($P < 0.05$ at 120 min) in the presence of calcium ionophore (stimulus) **(Figure. 5C)**. NETosis was similar in healthy, mannitol-treated (30 mM, osmostic control), and glucose-treated neutrophils (<20%) after 2 h in the absence of stimulus. However, NETosis was significantly upregulated (~70.5 ± 13.5 %) in glucose-treated neutrophils as

compared to controls (~30-40%, $P < 0.05$) when exposed to calcium ionophore **(Figure. 5D)**, which was consistent with earlier studies.[16,17,18] These results demonstrated the versatility of our developed technology for multiplexed neutrophil functional phenotyping (chemotaxis and NETosis) in a well-controlled microenvironment by changing the chemical stimulus in the reservoirs.

3. Discussion

In this work, we have developed a novel microfluidics platform for quantitative analysis of neutrophil chemotaxis and NETosis from whole blood directly. Neutrophils are isolated and enriched based on biomimetic cell margination and affinity-capture, followed by simultaneous on-chip functional phenotyping by exposure to pre-loaded chemical stimulus. We successfully validated the device performance using healthy and *in vitro* inflamed blood samples (TNF-α, high glucose), and demonstrated rapid risk stratification in a cohort of T2DM subjects. Key features of our technology include single-step user operation (sample loading), and direct neutrophil functional phenotyping without further sample processing (antibodies staining, cell lysis *etc.*). Moreover, the biochip reduces processing time from ~hours (using mL of blood) to a few minutes with small blood volumes (fingerprick), and only requires a syringe pump for device operation, which greatly facilitates point-of-care testing in clinical settings.

The most widely used chemotaxis assay is the transwell assay or Boyden chamber, where cells migrate across a microporous membrane in the presence of a concentration gradient, and subsequently counted to determine migration behavior. Chemotaxis chambers (Zigmond, Dunn, Insall) enable direct visualization of cells migration under well-defined chemical gradients, but

require single-cell tracking analysis with low throughput (~50 cells).[46] The developed microfluidic chemotaxis assay characterizes neutrophil migration and motility (velocity), which can yield useful clinical information in patients with burn injury[29] and asthma.[30] Unlike analysis of single-cell trajectories which is limited by the field-of-view during imaging,[28,47] the measured chemotaxis phenotypes are based on average or "bulk" neutrophil migratory behavior which do not require expensive microscopy system for time-lapse imaging, and offers the potential for performing multiple chemotaxis assays each time.

In our study, this multi-parametric phenotyping revealed distinct signature neutrophil migratory responses in blood treated with TNF-α and glucose. We showed that TNF-α-treated neutrophils had reduced cell migration and speed which was consistent with previous studies,[38] and glucose-treated neutrophils exhibited decreased migration but with similar chemotaxis velocities as healthy neutrophils. The mechanisms for the observed differences in neutrophil chemotaxis under different stimulus remain unclear and warrant further investigation. Possible explanations include the increase in integrin (CD11b)[10] which can affect chemotaxis,[48] regulation of fMLP receptors by TNF-α,[49] as well as the differential activation of Rac1 and Rac2 (members of the small Rho GTPase family) which can affect actin remodeling, chemotaxis and superoxide production in neutrophils.[50,51] These observed phenotypes is also determined based on a fraction (~200 – 500 cells) of the total neutrophil population, which is similar to other microfluidics assays, and shown to be representative of the overall functional differences in diseased state and during inflammation.[28,30] For better accuracy, we can increase the number or size of the side chambers to capture more neutrophils for chemotaxis assay. As the devices are usually prepared on the day of experiment, it is unclear whether long-term device storage will affect the pre-

loaded chemicals and antibodies functionalization. To further validate our method for clinical use, it is therefore important to address these practical issues to facilitate large-scale clinical testing.

T2DM is a chronic metabolic disorder characterized by hyperglycaemia, resulting in increased oxidative stress and low-grade inflammation. To our knowledge, this is the first demonstration using chemotaxis phenotyping for risk stratification, and immune-based functional assessment of drug efficacy *in vitro*. While we observed an overall neutrophil dysfunction in T2DM patients, their chemotaxis profiles were highly heterogeneous, which enabled us to further stratify them based on the severity of chemotaxis impairment. Despite the small sample size, our results showed that high-risk T2DM patients (characterized by low neutrophil migration and chemotaxis speed) were associated with higher CRP level ($P < 0.05$) and worse lipid metabolism than low-risk T2DM patients. These trends were indeed similar to earlier reports suggesting suppression of neutrophil chemotaxis with hyperglycemia,[14] as well as improved neutrophil chemotaxis in diabetic patients with lower cholesterol levels due to dietary supplementation.[52] Interestingly, we also observed differential effects of common diabetic drugs (pravastatin and metformin) on healthy neutrophil chemotaxis using our technology, and significant enhancement of neutrophil chemotaxis in T2DM patients after metformin treatment *in vitro*. This can be attributed to metformin-mediated 5' adenosine monophosphate-activated protein Kinase (AMPK) activation, [53] which has anti-inflammatory effects[41], and can help improve leukocyte oxidative stress[54] and impaired neutrophil functions to "healthy baseline" in T2DM. In addition, as we observed a differential behavior (reduced cell migration) in healthy neutrophils after *in vitro* metformin exposure, it is also important to compare the immunometabolism effects of metformin on neutrophils in normal glycemic (healthy) and hyperglycemia (T2DM) blood samples.

Nevertheless, our data clearly suggest the feasibility of the developed neutrophil profiling technology for T2DM testing. Future work includes large-scale clinical validation for specific applications including stratification of T2DM subjects at risk of infections based on innate immune status[12], and screening for sodium glucose co-transporter-2 (SGLT2) inhibitors medication, which is known to increase the risks for developing genital and urinary tract infections (UTIs) in T2DM.[55,56]

As proof-of-concept for multiplexed microfluidics neutrophil phenotyping, we loaded a NETosis stimulus in the side reservoirs of the developed biochip to induce NETs formation in the purified neutrophils. Blood samples were stained with a nuclear dye (Hoechst) and NETosis was quantified by monitoring distinct intracellular nucleus degradation over time. Moussavi-Harmi *et al.* recently reported a similar optical-based approach to study reactive oxygen species (ROS) production and NETosis in microfluidics,[32] and we further showed in this work that it facilitates rapid quantification and differentiation of healthy and glucose-treated neutrophils based on NETosis phenotype within 2 h. We anticipate this technology to be highly useful for characterizing early-stage intracellular NETosis processes, as well as profiling of patients at risk of developing NETosis-related complications. Of note, the chemotaxis and NETosis assays were performed separately to better evaluate the device performance in studying neutrophil functions. We also demonstrated the feasibility of characterizing both neutrophil functions within the same device by loading different reagents (chemicals) in the reservoirs **(Supplementary Figure. S8)**. The developed technology can also be further engineered to functionalize or load different chemicals in more side chambers for multi-parametric neutrophil functional testing (cell rolling

and cytokine release *etc.*) to provide a more comprehensive neutrophil profiling for immune risk stratification.

In summary, we have developed a novel microfluidic device for multiplexed neutrophil functional phenotyping using a drop of blood. The unique strategy of integrating neutrophil sorting with chemotaxis/NETosis assay offers several key advantages including rapid, single step neutrophil purification and enrichment (~10 min), and well-controlled microenvironment for inflammatory profiling. We envision this enabling technology can significantly aid characterization of neutrophil chemotaxis and NETosis, which can be further developed into novel surrogate biomarkers for risk stratification in T2DM. Clinically, this immune health testing method will provide new insights into the association between alterations of cardiovascular risk factors and neutrophil dysfunction, and enable proper identification of high-risk patients for timely interventions.

4. Experimental Section

Please refer to Supplementary information for detailed description of device fabrication and device preparation.

4.1. Device Operation

Prior to blood sample loading, RPMI 1640 media (Lonza) loaded in a 1 mL syringe was perfused through the device inlet at 5 μL min^{-1} for 5 min using a syringe pump (Chemyx). The syringe tubing was then detached and whole blood (10 μL) was loaded into the device inlet using a gel loading tip. The syringe tubing was reattached to perfuse the blood at 2 μL min^{-1}. As blood transverse through the microchannel, the leukocytes marginate to the channel sides and are sorted into the smaller side channels. Marginated neutrophils are subsequently captured on anti-CD66b functionalized side chambers. After all the blood sample has been processed, the

continuous perfusion of RPMI media will wash away any unspecific binding to yield a pure neutrophil population at the side chambers. The flow was then maintained at 0.2 μL min^{-1} to form a diffusion-based chemical gradient near the reservoir. The experiment was carried out in a live-cell incubator at 37°C with 5% CO_2 for 2 h. For chemotaxis assay, time-lapse images or phase contrast images were taken at the start and end of the experiment. For NETosis assay, whole blood was pre-stained with Hoechst 33342 nucleic acid stain (1 μg mL^{-1}, Life Technologies) for 30 min at room temperature for nucleus visualization, and fluorescence time-lapse images were taken every 60 s interval for 2 h, using MetaMorph software (Molecular Devices).

4.2. Neutrophil Treatment

To examine the effects of different inflammatory stimulus on neutrophil chemotaxis or NETosis, whole blood was treated with the prototypic pro-inflammatory cytokine TNF-α (10 ng mL^{-1}; Peprotech), high levels of D-glucose (30 mM; Sigma-Aldrich) or PMA (2 nM; Sigma-Aldrich) for 30 min at room temperature prior the experiment. Mannitol (30 mM; Sigma-Aldrich) was used as an osmotic control for D-glucose. To test the effect of established drugs mitigating cardiovascular risks, whole blood samples were incubated with the water soluble HMG-CoA reductase inhibitor pravastatin (20 μM, Merck) for 30 min or the AMP-kinase activator metformin hydrochloride (1 mM, Sigma-Aldrich) for 1 h at room temperature.

4.3. Study Approval

For all subjects, informed consent was obtained during recruitment. All protocols were approved by the institutional review boards of Nanyang Technological University (IRB-2014-04-27) and Tan Tock Seng Hospital (2014/00416), in compliance with the Human Biomedical Research Act (Ministry of Health, Singapore). For fingerprick blood sampling, capillary blood was obtained from healthy donors according to WHO guidelines (Capillary sampling, WHO Guidelines on Drawing Blood, 2019) using a disposable lancet (Roche Diagnostics Corp.) and collected in EDTA tubes (BD Microtainer). A total of 12 T2DM male subjects with Chinese or Indian ethnicity were recruited (Table S1). ~2.5 to 3 mL of blood was collected by venepuncture into EDTA vacutainer (BD Biosciences) and processed on the same day for microfluidics experiments.

4.4. Statistical Analysis

All numerical data were expressed as mean ± standard error (s.e.m.) unless specified otherwise. We assessed the statistical significance of the difference between two sets of data using Mann-Whitney test (unless specified otherwise) with $P < 0.05$ to be considered of significant difference. All analysis was performed using GraphPad Prism V5.0 (GraphPad Software).

Supporting Information
Supporting Information is available from the Wiley Online Library or from the author.

Acknowledgements
B.O.B. is supported by the Lee Kong Chian School of Medicine, Nanyang Technological University Start Up Grant, MOE AcRF Tier 1 (2015-T1-001-258) and NTU-NHG Metabolic Diseases Collaboration Grant (MDCG/15006). H. W. H would like to acknowledge support from the Lee Kong Chian School of Medicine (LKCMedicine) Postdoctoral Fellowship, NTU-NHG Metabolic Diseases Collaboration Grant (MDCG/15004), as well as the Singapore Ministry of Health's National Medical Research Council under <CBRGNIG (NMRC/BNIG/2038/2015>.

Author contributions

H.W.H and H.M.T designed research. H.W.H and H.M.T performed experiments and analyzed the data. H.W.H, H.M.T, R.D, K.H.H.L. and B.O.B wrote the manuscript. All authors reviewed the manuscript.

Received: ((will be filled in by the editorial staff))
Revised: ((will be filled in by the editorial staff))
Published online: ((will be filled in by the editorial staff))

References

[1] S. Wild, G. Roglic, A. Green, R. Sicree, H. King, *Diabetes Care* **2004**, 27, 1047.
[2] C. D. A. Stehouwer, M.-A. Gall, J. W. R. Twisk, E. Knudsen, J. J. Emeis, H.-H. Parving, *Diabetes*, **2002**, 51, 1157.
[3] A. D. Pradhan, J. E. Manson, N. Rifai, J. E. Buring, P. M. Ridker, *JAMA* **2001**, 286, 327-334.
[4] J. C. Pickup, *Diabetes Care* **2004**, 27, 813.
[5] G. Silbernagel, M. E. Kleber, T. B. Grammer, B. R. Winkelmann, B. O. Boehm, W. März, *Diabetes Care* **2011**, 34, 2471.
[6] T. C. Alba-Loureiro, C. D. Munhoz, J. O. Martins, G. A. Cerchiaro, C. Scavone, R. Curi, P. Sannomiya, *Braz. J. Med. Biol. Res.* **2007**, 40, 1037.
[7] B. Menart-Houtermans, R. Rütter, B. Nowotny, J. Rosenbauer, C. Koliaki, S. Kahl, M.-C. Simon, J. Szendroedi, N. C. Schloot, M. Roden, *Diabetes Care* **2014**, 37, 2326.
[8] E. Ernst, A. Matrai, *Diabetes* **1986**, 35, 1412.
[9] Z. Pécsvarády, T. C. Fisher, C. H. Darwin, A. Fabók, T. S. Maqueda, M. F. Saad, H. J. Meiselman, *Diabetes Care* **1994**, 17, 57-63.
[10] H. W. Hou, C. Petchakup, H. M. Tay, Z. Y. Tam, R. Dalan, D. E. K. Chew, K. H. H. Li, B. O. Boehm, *Sci. Rep.* **2016**, 6, 29410.
[11] J. D. Bagdade, R. K. Root, R. J. Bulger, *Diabetes* 1**974**, 23, 9.
[12] B. R. Shah, J. E. Hux, *Diabetes Care* **2003**, 26, 510.
[13] A. G. Mowat, J. Baum, *N. Engl. J. Med.* **1971**, 284, 621.
[14] M. Delamaire, D. Maugendre, M. Moreno, M. C. Le Goff, H. Allannic, B. Genetet, *Diabetic Med.* **1997**, 14, 29.
[15] V. Brinkmann, U. Reichard, C. Goosmann, B. Fauler, Y. Uhlemann, D. S. Weiss, Y. Weinrauch, A. Zychlinsky, *Science* **2004**, 303, 1532.
[16] L. Menegazzo, S. Ciciliot, N. Poncina, M. Mazzucato, M. Persano, B. Bonora, M. Albiero, S. Vigili de Kreutzenberg, A. Avogaro, G. P. Fadini, *Acta Diabetol.* **2015**, 52, 497-503.
[17] S. L. Wong, M. Demers, K. Martinod, M. Gallant, Y. Wang, A. B. Goldfine, C. R. Kahn, D. D. Wagner, *Nat. Med.* **2015**, 21, 815.
[18] G. P. Fadini, L. Menegazzo, M. Rigato, V. Scattolini, N. Poncina, A. Bruttocao, S. Ciciliot, F. Mammano, C. D. Ciubotaru, E. Brocco, M. C. Marescotti, R. Cappellari, G. Arrigoni, R. Millioni, S. Vigili de Kreutzenberg, M. Albiero, A. Avogaro, *Diabetes* **2016**, 65, 1061.

[19] K. T. Kotz, W. Xiao, C. Miller-Graziano, W.-J. Qian, A. Russom, E. A. Warner, L. L. Moldawer, A. De, P. E. Bankey, B. O. Petritis, D. G. Camp, A. E. Rosenbach, J. Goverman, S. P. Fagan, B. H. Brownstein, D. Irimia, W. Xu, J. Wilhelmy, M. N. Mindrinos, R. D. Smith, R. W. Davis, R. G. Tompkins, M. Toner, *Nat. Med.* **2010**, 16, 1042.
[20] S. M. Prakadan, A. K. Shalek, D. A. Weitz, *Nat. Rev. Genet.* **2017**, 18, 345.
[21] B. Kim, M. Wu, *Ann. Biomed. Eng.* **2012**, 40, 1316.
[22] F. Lin, C.-C. Nguyen, S.-J. Wang, W. Saadi, S. Gross, N. Jeon, *Ann. Biomed. Eng.* **2005**, 33, 475.
[23] C. N. Jones, J. Dalli, L. Dimisko, E. Wong, C. N. Serhan, D. Irimia, *Proc. Natl. Acad. Sci. U. S. A.* **2012**, 109, 20560.
[24] L. Boneschansker, J. Yan, E. Wong, D. M. Briscoe, D. Irimia, *Nat. Comm.* **2014**, 5, 4787.
[25] F S. Fukuda, G. W. Schmid-Schönbein, *J. Leukocyte Biol.* **2002**, 72, 133.
[26] A. N. Hoang, C. N. Jones, L. Dimisko, B. Hamza, J. Martel, N. Kojic, D. Irimia, *Technology* **2013**, 1, 49.
[27] N. Agrawal, M. Toner, D. Irimia, *Lab Chip* **2008**, 8, 2054
[28] E. K.-H. Sackmann, E. Berthier, E. W. K. Yong, M. A. Shelef, S. A. Wernimont, A. Huttenlocher and D. J. Beebe, *Blood* **2012**, 120, e45.
[29] K. L. Butler, V. Ambravaneswaran, N. Agrawal, M. Bilodeau, M. Toner, R. G. Tompkins, S. Fagan, D. Irimia, *PLoS One* **2010**, 5, e11921.
[30] E. K.-H. Sackmann, E. Berthier, E. A. Schwantes, P. S. Fichtinger, M. D. Evans, L. L. Dziadzio, A. Huttenlocher, S. K. Mathur, D. J. Beebe, *Proc. Natl. Acad. Sci. U. S. A.* **2014**, 111, 5813.
[31] L. Barrientos, V. Marin-Esteban, L. de Chaisemartin, V. Lievin le moal, C. Sandre, E. Bianchini, V. Nicolas, M. Pallardy and S. Chollet-Martin, *Front. Immunol.* **2013**, 4.
[32] S. F. Moussavi-Harami, K. M. Mladinich, E. K. Sackmann, M. A. Shelef, T. W. Starnes, D. J. Guckenberger, A. Huttenlocher, D. J. Beebe, *Integr. Biol.* **2016**, 8, 243.
[33] H. W. Hou, A. A. S. Bhagat, A. G. L. Chong, P. Mao, K. S. W. Tan, J. Han and C. T. Lim, *Lab Chip* **2010**, 10, 2605.
[34] H. W. Hou, H. Y. Gan, A. A. S. Bhagat, L. D. Li, C. T. Lim and J. Han, *Biomicrofluidics* **2012**, 6, 024115.
[35] H. L. Goldsmith, G. R. Cokelet and P. Gaehtgens, *Am. J. Physiol.: Heart Circ. Physiol.* **1989**, 257, H1005.
[36] H. W. Hou, L. Wu, D. P. Amador-Munoz, M. P. Vera, A. Coronata, J. A. Englert, B. D. Levy, R. M. Baron and J. Han, *Lab Chip* **2016**, 16, 688.
[37] S. M. Davidson, O. Jonas, M. A. Keibler, H. W. Hou, A. Luengo, J. R. Mayers, J. Wyckoff, A. M. Del Rosario, M. Whitman, C. R. Chin, K. J. Condon, A. Lammers, K. A. Kellersberger, B. K. Stall, G. Stephanopoulos, D. Bar-Sagi, J. Han, J. D. Rabinowitz, M. J. Cima, R. Langer and M. G. Vander Heiden, *Nat. Med*. **2017**, 23, 235.
[38] K. L. Vollmer, J. S. Alberts, H. T. Carper and G. L. Mandell, *J. Leukocyte Biol.* **1992**, 52, 630-636.
[39] B. Wierusz-Wysocka, H. Wysocki, A. Wykrętowicz and R. Klimas, *Acta Diabetol. Lat.* **1988**, 25, 283.
[40] K. A. Deans and N. Sattar, *Diabetes Technol. Ther.* **2006**, 8, 18.
[41] D. W. Park, S. Jiang, J.-M. Tadie, W. S. Stigler, Y. Gao, J. Deshane, E. Abraham and J. W. Zmijewski, *Mol. Med.* **2013**, 19, 387.

[42] S. Dunzendorfer, D. Rothbucher, P. Schratzberger, N. Reinisch, C. M. Kähler and C. J. Wiedermann, *Circ. Res.* **1997**, 81, 963.
[43] B. Wierusz-Wysocka, H. Wysocki, H. Siekierka, A. Wykretowicz, A. Szczepanik and R. Klimas, *J. Leukocyte Biol.* **1987**, 42, 519.
[44] P. M. Ridker , C. H. Hennekens , J. E. Buring and N. Rifai, *N. Engl. J. Med.* **2000**, 342, 836.
[45] V. Brinkmann, C. Goosmann, L. I. Kühn and A. Zychlinsky, *Front. Immunol.* **2012**, 3, 413.
[46] A. J. Muinonen-Martin, D. M. Veltman, G. Kalna and R. H. Insall, *PLoS One* **2010**, 5, e15309.
[47] G. A. Wright, L. Costa, A. Terekhov, D. Jowhar, W. Hofmeister and C. Janetopoulos, *Microsc Microanal.* **2012**, 18, 816.
[48] C. Wang, H. Hayashi, R. Harrison, B. Chiu, J. R. Chan, H. L. Ostergaard, R. D. Inman, J. Jongstra, M. I. Cybulsky and J. Jongstra-Bilen, *J. Immunol.* **2002**, 169, 415.
[49] Y. H. Atkinson, W. A. Marasco, A. F. Lopez, and M. A. Vadas *J. Clin. Invest.* **1988**, 81, 759.
[50] H. Zhang, C. Sun, M. Glogauer and G. M. Bokoch, *J. Immunol.* **2009,** 183, 2718.
[51] C. X. Sun, G. P. Downey, F. Zhu, A. L. Y. Koh, H. Thang and M. Glogauer, *Blood* **2004**, 104, 3758.
[52] E. B. Schmidt, P. J. SØRensen, J. O. Pedersen, C. Jersild, J. Ditzel, N. Grunnet and J. Dyerberg, *J. Intern. Med.* **1989**, 225, 201.
[53] M. M. Mihaylova and R. J. Shaw, *Nat Cell Biol* **2011**, 13, 1016.
[54] N. Diaz-Morales, S. Rovira-Llopis, C. Bañuls, S. Lopez-Domenech, I. Escribano-Lopez, S. Veses, A. Jover, M. Rocha, A. Hernandez-Mijares and V. M. Victor, *Antioxid. Redox Signaling* **2017**.
[55] J. Liu, L. Li, S. Li, P. Jia, K. Deng, W. Chen and X. Sun *Sci. Rep.* **2017**, 7, 2824.
[56] S. Geerlings, V. Fonseca, D. Castro-Diaz, J. List, and S. Parikh, *Diabetes Res. Clin. Pract.* **2014**, 103, 373.

Figures and figure legends

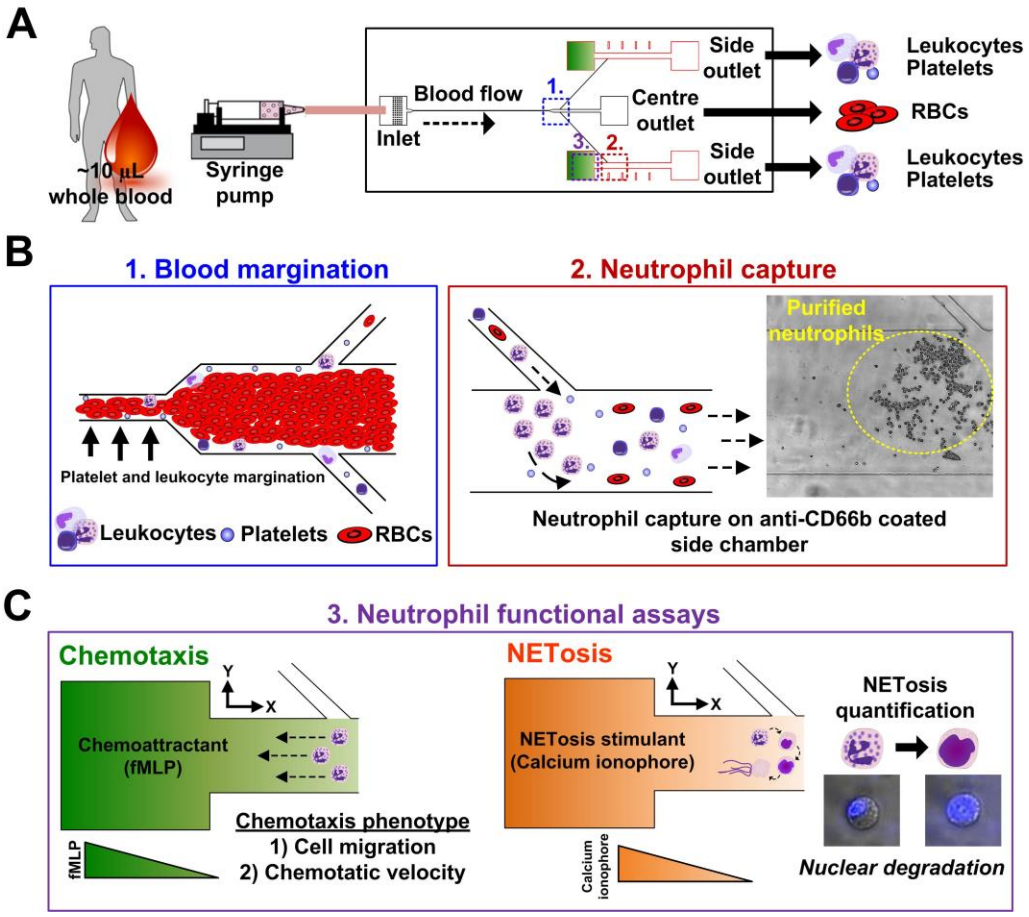

Figure 1. Integrated point-of-care neutrophil purification and phenotyping using microfluidics. (A) Microdevice design and setup for neutrophil sorting and functional characterization using small blood volumes (~10 µL). **(B)** Schematic illustration of neutrophil purification. As whole blood flows through the margination channel (20 µm (*w*) × 20 µm (*h*)), red blood cells (RBCs) undergo axial migration towards the channel centre, which result in leukocytes and platelets margination to the channel sides (stage 1). Neutrophils sorted into the smaller side channels are selectively captured on anti-CD66b (neutrophil specific ligand) functionalized surfaces at the side chambers (stage 2). Representative brightfield image indicates enriched neutrophils after washing. **(C)** Schematic illustration of neutrophil functional assay. Purified neutrophils are subsequently exposed to either preloaded chemoattractant N-Formylmethionyl-leucyl-phenylalanine (fMLP, 200 nM), or calcium ionophore (20 µM) in the reservoirs for on-chip chemotaxis and formation of neutrophil extracellular traps (NETosis) assay, respectively (stage 3).

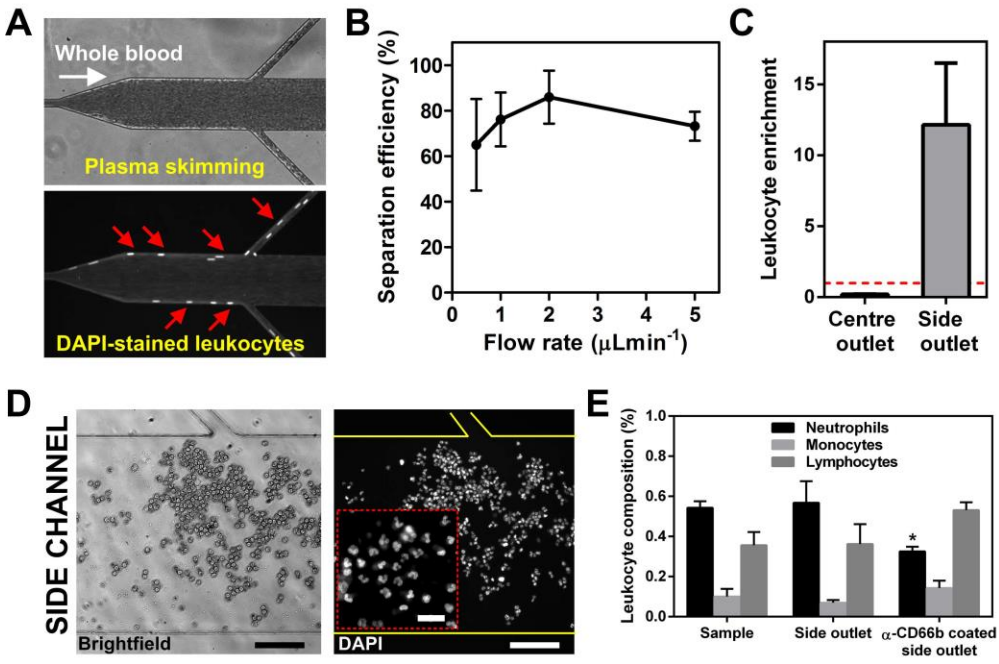

Figure 2. Neutrophil sorting and purification from whole blood directly. (A) Representative brightfield and fluorescent images at the end of the margination channel indicating plasma skimming and leukocyte margination (red arrows) effects. **(B)** Leukocyte separation efficiency into the side channels at different flow conditions. **(C)** Significant leukocyte enrichment (~12-fold) was achieved at the side outlet at 2 μL min^{-1}. Red dotted line (value of 1) indicates normalized inlet sample leukocyte concentration. **(D)** Representative brightfield and fluorescent images at the side chambers showing effective neutrophil capture near the connecting side channel (Scale bar: 100 μm). Enlarged image (inset) highlights distinct multi-lobed nucleus in purified neutrophils stained with nuclear dye (Hoechst) (Scale bar: 20 μm). **(E)** Significant depletion of neutrophils in the eluent from the side outlet coated with anti-CD66b antibodies. *P<0.05 versus sample inlet and uncoated side outlet.

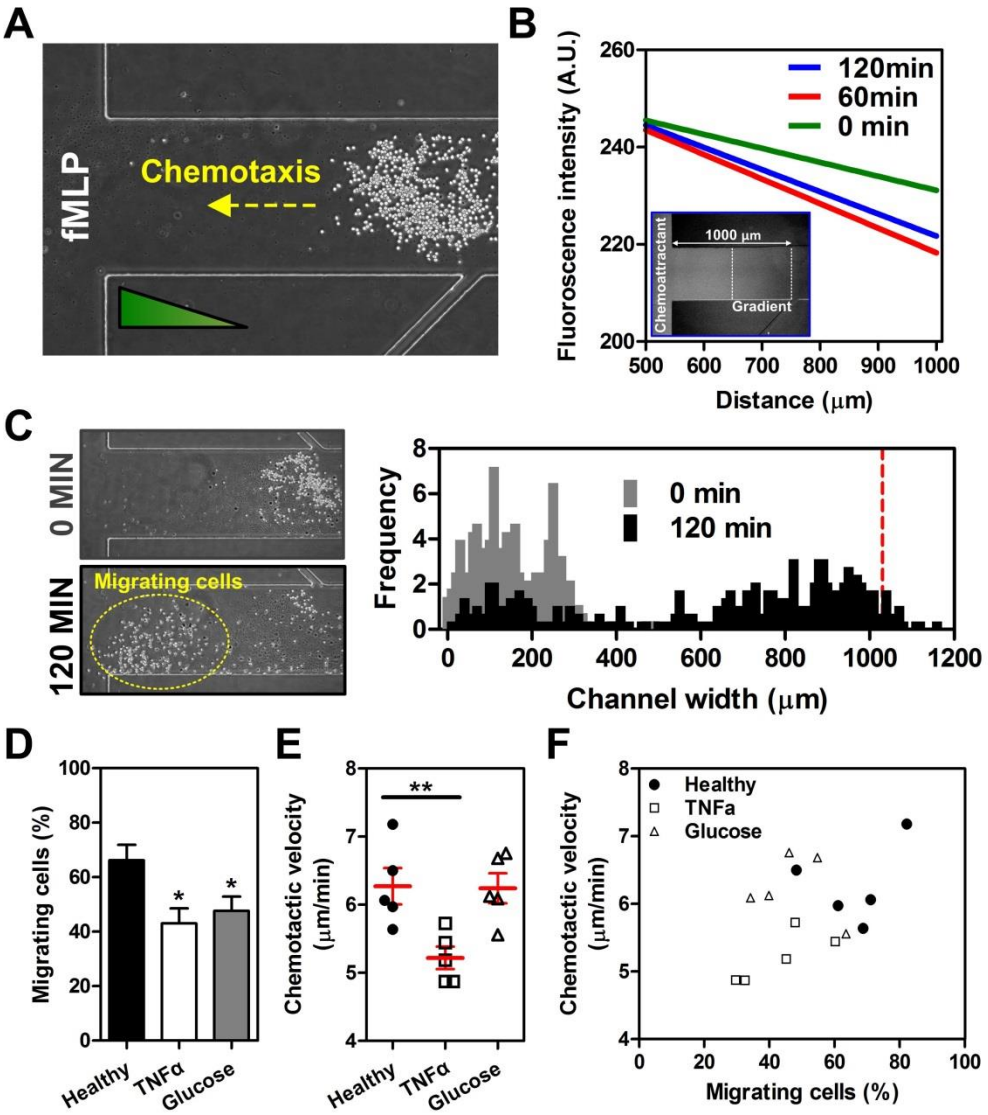

Figure 3. On-chip neutrophil chemotaxis assay. (A) Representative brightfield image indicating significant neutrophils capture at the side channel proximal to the chamber preloaded with chemoattractant (fMLP, Mr~438Da). **(B)** Formation of linear FITC (Mr~390Da) concentration gradient within the chemotaxis assay (dotted) region. Inset fluorescence image corresponds to stable FITC diffusion after 2 h. **(C)** Brightfield images and histogram distribution plot indicating neutrophil chemotaxis towards fMLP. Red dotted line represents the boundary of the chemoattractant chamber. Quantification of **(D)** neutrophil migration, **(E)** chemotaxis velocity with different inflammatory stimulus (TNF-α (10 ng mL^{-1}) and glucose (30 mM)). **(F)** 2D scatter plot indicating distinct chemotaxis behavior for healthy, TNF-α and glucose-treated neutrophils. *P<0.05 and **P<0.01 versus untreated (healthy) condition.

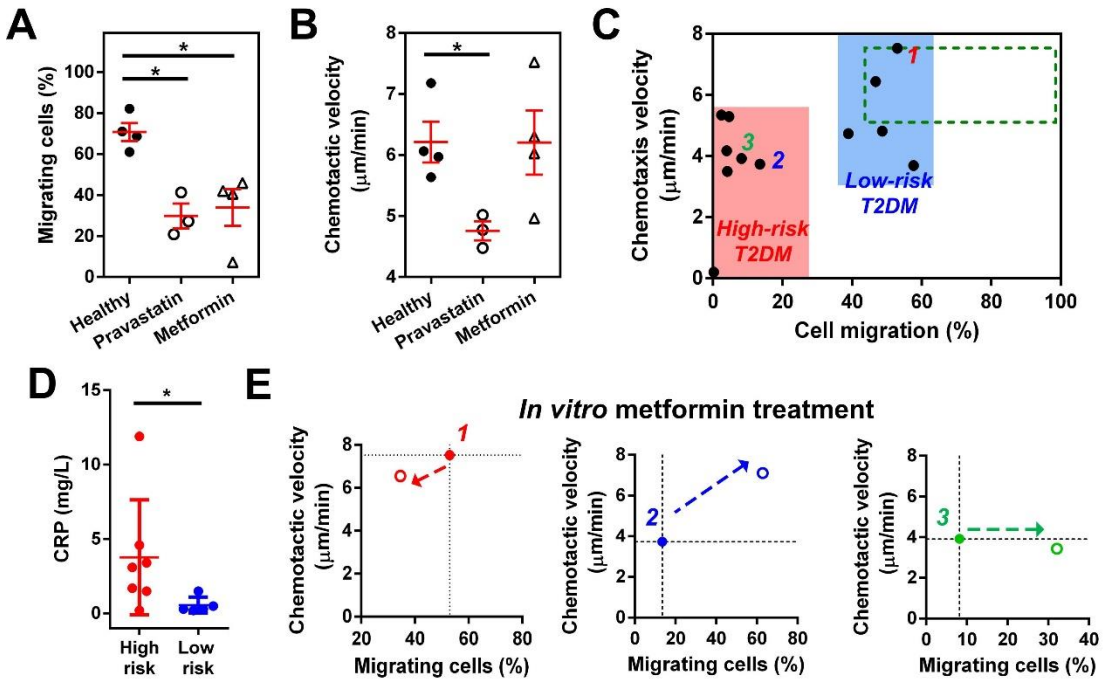

Figure 4. Clinical applications of the microfluidic chemotaxis assay in T2DM. Characterization of **(A)** neutrophil migration and **(B)** chemotaxis velocity in whole blood treated with different diabetic drugs (pravastatin (10 nM) and metformin (1 μM)) *in vitro*. **(C)** Scatter plot of neutrophil chemotactic phenotype in T2DM patients (n = 12). Green dashed box indicates chemotaxis region for healthy neutrophils (*see methods*). T2DM subjects are sub-grouped into high-risk (red box) and low-risk (blue box) based on chemotaxis attenuation. **(D)** Higher C-reactive protein (CRP) level was observed in high-risk T2DM patients. **(E)** Mitigation of chemotaxis behavior in T2DM patients (n = 3) after blood treatment with metformin *in vitro*. Corresponding patients (1 to 3) are indicated in (C). *P<0.05.

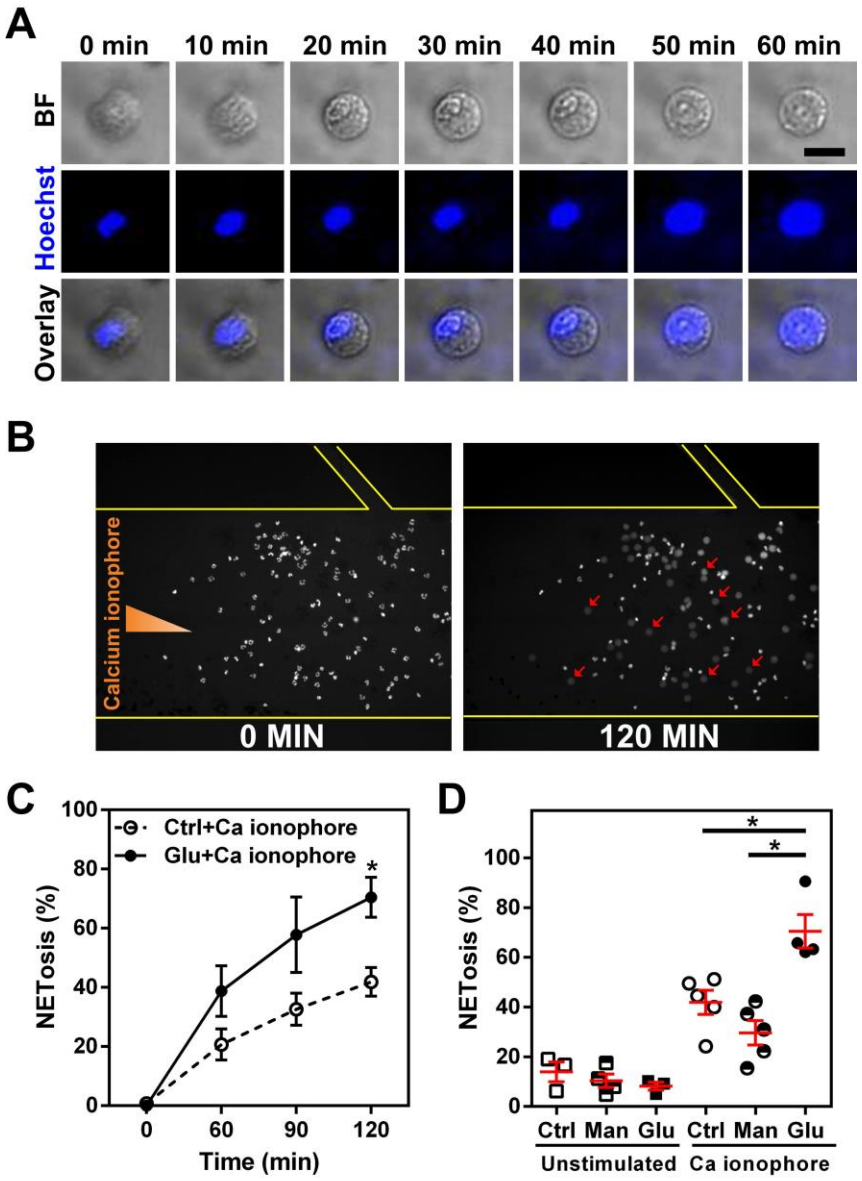

Figure 5. On-chip NETosis assay. (A) Representative brightfield, fluorescence (Hoechst) and overlaid images illustrating nucleus degradation and leakage of DNA content into cytoplasm of a neutrophil undergoing NETosis in 60 min. Scale bar: 10 µm. **(B)** Fluorescence images of the side channel at the start (0 min) and end (120 min) of the NETosis assay. Neutrophils undergoing NETosis (red arrows) was observed after 2 h of exposure to NETs stimulus (calcium ionophore). **(C)** Quantification of NETs formation over time in healthy (untreated) and glucose-treated (30 mM) neutrophils. **(D)** Characterization of NETosis in untreated (control), mannitol- (30 mM, osmotic control) and glucose-treated (30mM) neutrophils with and without calcium ionophore stimulation. *P<0.05.